3

Chaos and Intermittency in an Endocrine System Model

Ralph H. Abraham
Mathematics Board
University of California
Santa Cruz, California

Hüseyin Koçak
Lefschetz Center for Dynamical Systems
Brown University
Providence, Rhode Island

William R. Smith
Department of Mathematics and Statistics
University of Guelph
Guelph, Ontario, Canada

A modification to a response-inhibition model for the hypothalamic-pituitary-gonadal axis of the male reproductive system gives rise to two periodic attractors in a bifurcation diagram exhibiting hysteresis and intermittency. This is interpreted as a possible model for differential hormonal release, system disorders and noise amplification in the endocrine system. The modification includes a response of the hypothalamus to short feedback.

1. INTRODUCTION

Earlier systems of differential equations modeling the male mammalian reproductive endocrine system have exhibited a Hopf bifurcation (Smith, 1981). The basic model consisted of a negative feedback system of three ordinary differential equations. The bifurcation parameter is a counterpart of biological age, and it was suggested that the onset of the limit cycle qualitatively mimics the onset of puberty. Experimental data obtained from laboratory animals display noisy almost-periodic time series, however. In a recent paper, a modification was made to one of the feedback functions for such a dynamical system (corresponding in our model

to response of the hypothalamus to testosterone, which we call long feedback). This produced a chaotic attractor, in the sense of probability at least, in place of the limit cycle (Rössler, Gotz, and Rössler, 1979; see also Sparrow, 1981). This could be useful in adapting the model to better mimic the data, which is characteristically noisy. However, this modification of the long feedback function (raising the skirt to a V shape) is difficult to interpret physiologically.

In this paper, we achieve a similar result with different modifications of the model. First, the V-shaped modification to the long feedback function is replaced by a slight kink. The chaotic probable-attractor persists, as shown in Appendix B. With a second modification, based on the concepts of complex dynamical systems theory (Abraham, 1982a, 1982b, 1982c), we introduce a response of the hypothalamus to the pituitary hormone, which we call short feedback. Then, in an extensive series of simulations, we discover a second periodic attractor, shown in Appendix C, and a rich bifurcation diagram, indicated in Appendix D.

2. THE BASIC SYSTEM FOR LONG FEEDBACK

Here we review the simple model which exhibits a Hopf bifurcation. In this model, the endocrine system consists of three hormonal sources: the hypothalamus (H), the pituitary (P), and the gonads (G). Each of these emits a single hormone: luteinizing-hormone releasing hormone(R) from H, luteinizing hormone(L) from P, and testosterone(T) from G. We represent the appropriate serum concentration of each (normalized or rescaled values, relative to standard levels) by x, y, z, respectively. The domain of the basic dynamical system is Euclidean three-space, with these relative concentrations as coordinates. The system of first-order equations for the rates of secretion of the three hormones into the relevant circulatory systems represents the long feedback loop of Figure 1. The basic equations are:

$$\begin{aligned} \dot{x} &= f(z) - x \\ \dot{y} &= h(x) - y \\ \dot{z} &= g(y) - z \end{aligned} \tag{1}$$

Choosing the simplest forms for the three stimulus-response (S-R) functions f, h, and g (as shown in Fig. 2), a Hopf bifurcation is obtained

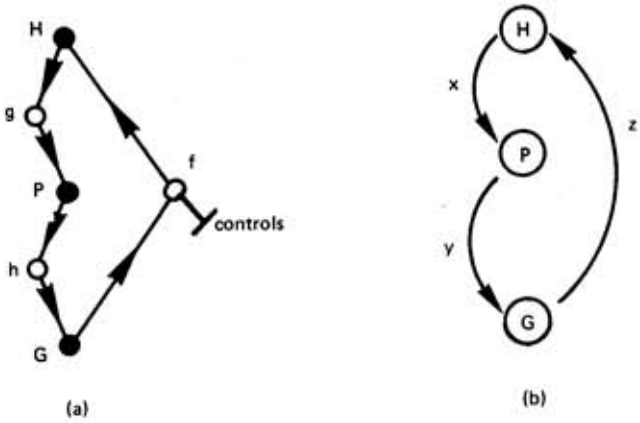

FIGURE 1. THE LONG FEEDBACK CYCLE.
(a) schematic diagram (b) pictorial diagram

in system (1) by varying the parameter a. We regard this parameter as a control of the static coupling function, f. The other parameter, f[0], is held fixed.

The basic system is physiologically more plausible if all three S-R functions are smooth ramps (Michaelis-Menten functions). For ease of digital simulation, we shall use piecewise-linear ramps for our improved basic system, shown in Fig. 3. This improved basic system exhibits the same qualitative features as the original basic system. The trajectories are shown in Figs. A1 and A2 in Appendix A. The traditional analysis is summarized here for review.

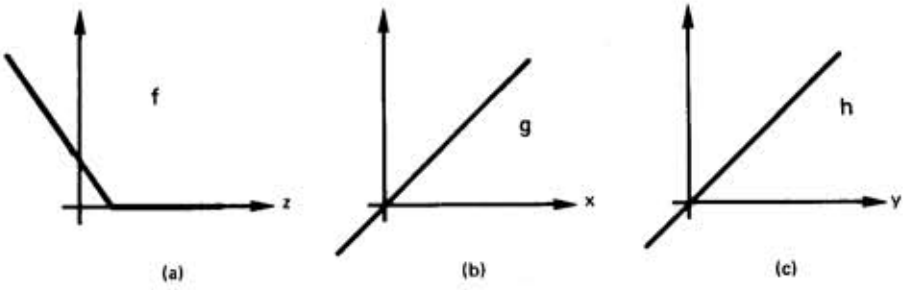

FIGURE 2. THE SIMPLEST S-R FUNCTIONS OF THE BASIC SYSTEM.

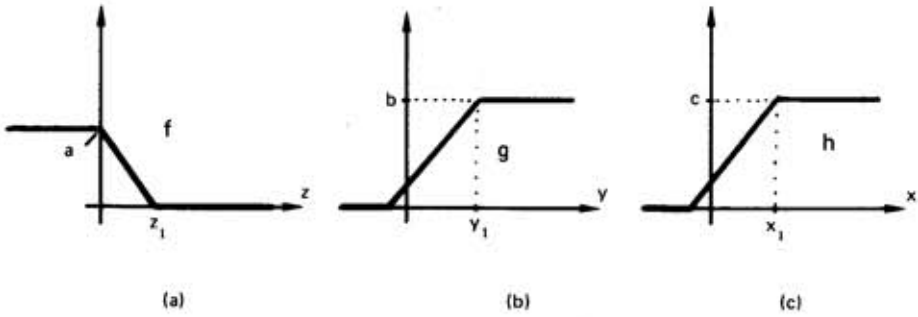

FIGURE 3. PIECEWISE-LINEAR RAMP S-R FUNCTION OF THE IMPROVED BASIC SYSTEM.

We begin by looking for the critical points of the improved basic system. Setting the three rates to zero, we have:

$$\begin{aligned} x &= f(z) \\ y &= h(x) \\ z &= g(y) \end{aligned} \tag{2}$$

or, equivalently,

$$x = f(g[h(x)]) = F(x), \tag{3}$$

where F = fogoh, which we shall call the zero discriminant function. Zeroes of the vector field are revealed as fixed points of this function, or equivalently, as intersections of its graph with the diagonal, D = {x,x}.

In the original system (Figure 2) with g and h equal to the identity, F is equal to f, and is monotone decreasing, as shown in Figure 4a. In the improved system (Figure 3), F is still monotone, as shown in Figures 4b and 4c. The toe of F at $x = x_1$ occurs at the smallest of the three saturation stimuli, so even in the improved system (Figure 3), all three cases of Fig. 4 are possible. In each, however, there is only one crossing of the diagonal, D, at $x = x_0$. Thus $F(x_0) = D(x_0) = x_0$, and x_0 determines the unique critical point of the improved system,

$$p_0 = (x_0\ y_0,\ z_0) = (x_0,\ h[x_0],\ g(h(x_0)) \tag{4}$$

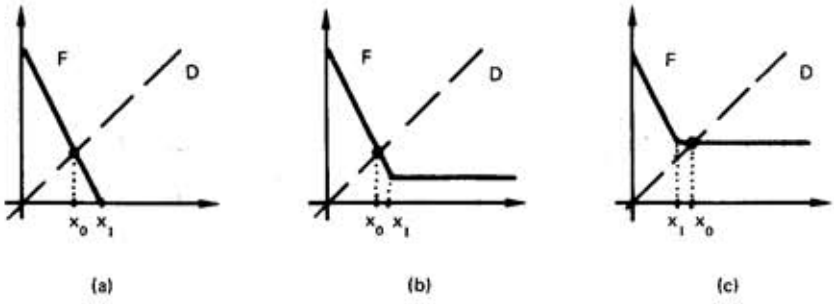

FIGURE 4. THE ZERO DISCRIMINANT FUNCTION.

Assuming that this point is typical (that is, not at a joint of f, g, or h), then the system is linear at p_0. Or, if we put

$$\begin{aligned} X &= x - x_0 \\ Y &= y - y_0 \\ Z &= z - z_0 \end{aligned} \tag{5}$$

the system becomes

$$\begin{aligned} X' &= -aZ - X \\ Y' &= cX - Y \\ Z' &= bY - Z \end{aligned} \tag{6}$$

or, in matrix notation, $P' = AP$

where

$$A = \begin{vmatrix} -1 & 0 & -a \\ c & -1 & 0 \\ 0 & b & -1 \end{vmatrix} \tag{7}$$

A has eigenvalues, $(-abc)^{1/3} - 1$, as shown in Figure 5. If $m = 1$, we get a Hopf bifurcation, so we exclude this case (see Fig. 4a(cube root)) and increase the radius, m, via a, b, or c.

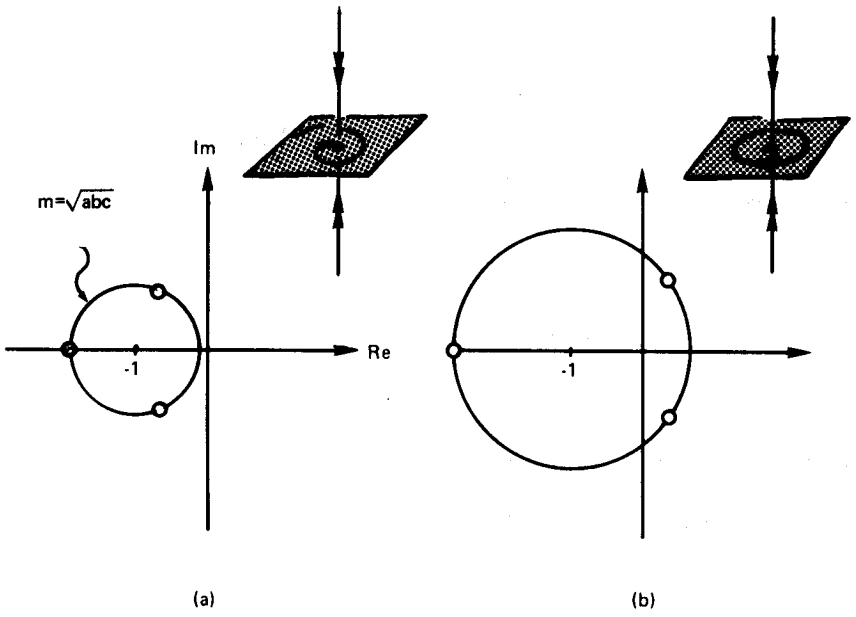

FIGURE 5. CHARACTERISTIC EXPONENTS.

The spectrum of A, with corresponding phase portraits.

(a) Rest point, small m (b) Oscillation, large m

3. THE CHAOTIC ATTRACTOR

The modified long feedback reponse function introduced by Rössler, Gotz, and Rössler (1979), and used by them and by Sparrow (1981) to obtain a convergent sequence of bifurcations leading to a chaotic probable-attractor, is shown in Figure 6(a). The large rise to the right is not actually needed. We replace this by a piecewise linear form of the Michaelis-Menton S-R function, as in the basic model of the preceding section. This is shown in Figure 6(b). With the height of the skirt as a control parameter, the sequence of bifurcations still converges to a chaotic attractor. The details are shown in Appendix B. It may yet be unacceptable physiolgically but monotonicity is violated only in a very small region of hormone concentrations.

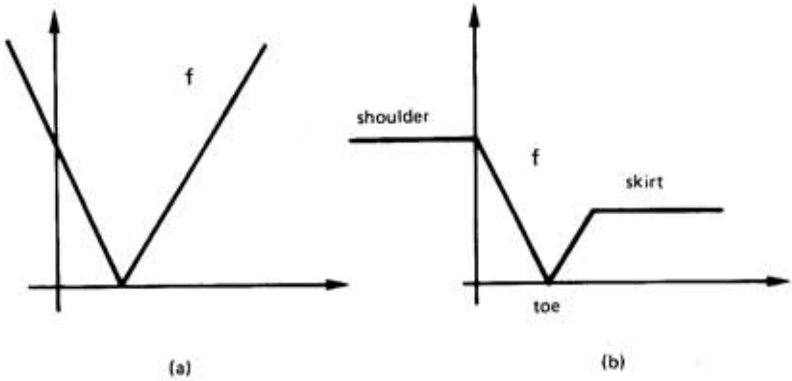

FIGURE 6. THE LONG FEEDBACK FUNCTIONS FOR CHAOS.

(a) The original V-function. (b) The modified function.

4. THE NEW MODEL WITH SHORT FEEDBACK

We now include short feedback between the hypothalamus and the pituitary, by supposing the hypothalamus (H) is sensitive to L, emitted by the pituitary (P), as well as to T from the gonads (G). Thus we replace the scheme of Figure 1 by the modified one of Figure 7, and add the new

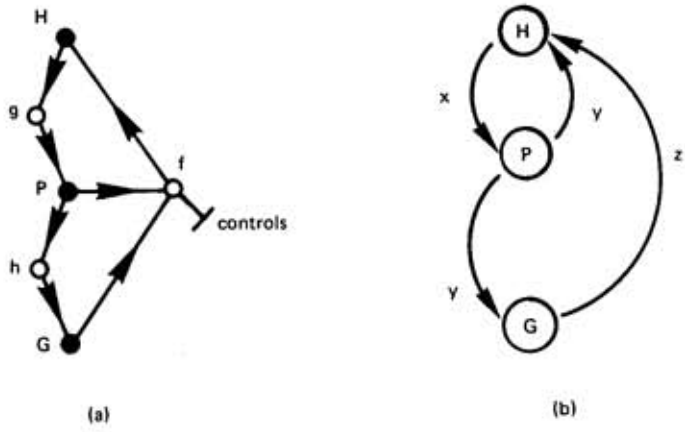

FIGURE 7. THE MODIFIED SCHEME WITH SHORT FEEDBACK.

(a) Schematic (b) Pictorial

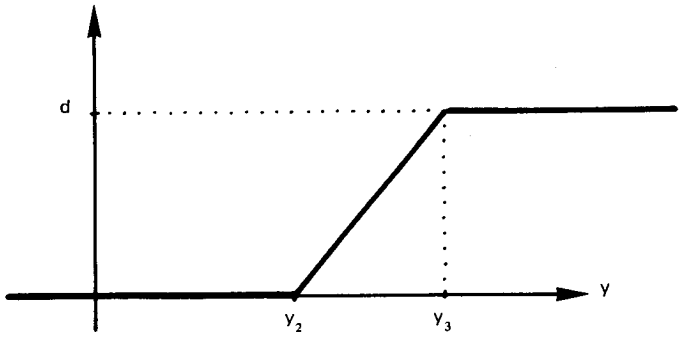

FIGURE 8. THE SHORT FEEDBACK FUNCTION.

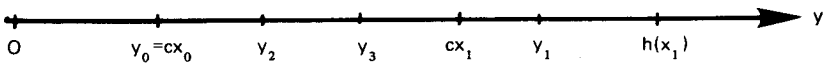

(a)

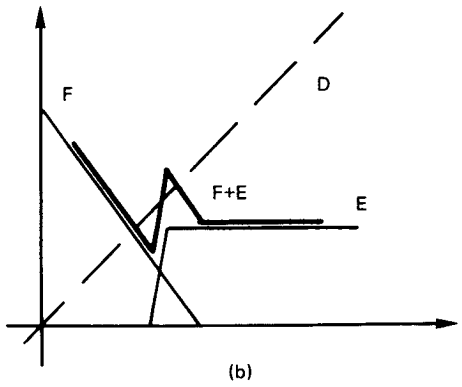

(b)

FIGURE 9. ZEROS OF THE MODIFIED SYSTEM.

(a) Choice of constants (b) Zero discriminant

response function, e(y) to the x equation. We assume the new S-R function, e, is a piecewise-linear ramp, like f, g, and h, as shown in Figure 8, obtaining the modified system,

$$\begin{aligned} \dot{x} &= e(y) + f(z) - x \\ \dot{y} &= h(x) - y \\ \dot{z} &= g(y) - z \end{aligned} \tag{8}$$

Seeking critical points as before, we see that (x_0,y_0,z_0) is a critical point of the system (8) only if $y_0 = h(x_0)$, $z_0 = g(y_0)$, and $x_0 = G(x_0)$, where:

$$G(x) = f(g\ [h(x)]) + e(h[x]) = F(x) + E(x)$$

Unlike that for F previously, G is no longer monotone. We will suppose the parameters of the functions are related as shown in Figure 9a. Then the graphs of E and F are as in Figure 9b. The toe joint, y_2, shoulder joint, y_3, and height, d, of the new sensitivity function, e, now join the height, a, and toe, b, of the original function, f, as the control parameters of the static coupling function, f+e.

5. THE TWO PERIODIC ATTRACTORS

We first fix the function f as one which provides a periodic attractor in the basic model of Section 2, as shown in Fig. A2. We next choose appropriate values for the toe and shoulder joints of the new response function, e. Then, regarding the height of e as the sole control parameter of the coupling function to the hypothalamus, simulation reveals the bifurcation diagram of the double fold catastrophe. A similar result has been discovered in a sequence of enzymatic reactions (Decroly and Goldbeter, 1982).

The actual trajectories are shown in the sequence of computer drawings in Appendix C. This diagram has been described in great detail as a model for intermittency and noise amplification (Abraham, 1983a). Here is the idea. Reducing the three-dimensional state space of the endocrine system fictitiously to one (for example, by observing only the amplitude of the oscillations) we may portray this bifurcation diagram in a plane, as shown in Fig. 10.

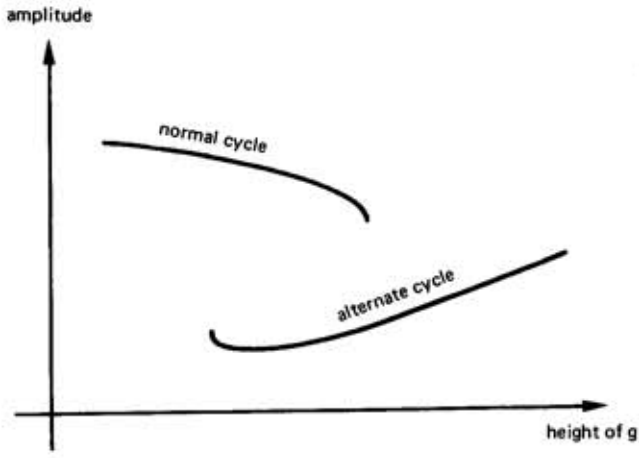

FIGURE 10. PERIODIC DOUBLE FOLD CATASTROPHE.

Increasing the control parameter from the far left across both bifurcation points, we observe a catastrophic change from the normal cycle to the alternate cycle at the right bifurcation point. Returning the control to its original value, we observe a catastrophic return to the normal cycle at the left bifurcation point. This is a hysteresis loop in the control space. If, for example, the control parameter were determined by another dynamical system, we might observe changes between the two cycles intermittently. This provides a model for intermittency in the context of serially coupled dynamical systems. In this particular case, both of the states intermittently occupied are periodic.

Now suppose that the scale of the amplitude (vertical) axis in Figure 10, relative to the control (horizontal) scale, is small. Thus, a very small oscillation in the control parameter results in a relatively large alternation between the normal and alternate cycles. Further, a small but noisy variation of the control parameter crossing both bifurcation points repeatedly results in a large and noisy variation between the two cycles. This is a model for noise amplification in the context of serially coupled dynamical systems. We see in Appendix C that in our modified model for the endocrine system, this exaggerated scale relationship applies. Small changes in the control parameter (height of the skirt between 0.70 and 0.95) produce a large, hysterical variation between the normal cycle and the alternate state. The magnitude of this variation is clearly shown in Figure C2(e).

6. APPLICATIONS TO THE PHYSIOLOGICAL SYSTEM

Suppose that in Fig. 10, the upper attractrix corresponds to the normal cycle exhibited in adults. The lower attractrix is an oscillation of smaller amplitude, and totally different period. This suggests three different possible physiological implications.

First, it is known that the hormone R effects the release of another hormone, follicle-stimulating hormone, from the pituitary in addition to L. The two different cycles of the model may correspond to the required stimuli for the release of the different hormones. The switching between the two release mechanisms would be effected by variations in the control parameter. This may thus be a mechanism for differential release of the different hormones.

Second, in view of the results of Appendix C, we see that amplification by the endocrine system of noise in the control parameter (sensitivity of H to R) could account for observed experimental noise in the serum concentration data of L and G.

As a third possible implication, suppose that the parameters in the model correspond to two different cycles, one characterizing the normal state, and the other a pathological state corresponding to some disorder. Then, based on the diagram, we may propose two therapeutic strategies. First, as dynamical systems latch on attractors, we may try to force the system from one attractor into the basin of the other, where it will then latch. Although catastrophic, this seems to have found some support in recent clinical findings (Jaffe, 1982). On the other hand, if a way were known to adjust the height parameter of the short feedback response function, e, of the hypothalamus to luteinizing harmonic, then a small, gradual, temporary decrease would achieve the same effect.

7. CUSP CATASTROPHES

We fix the basic response function, f, as above. Fixing the height of the new response function, e, at a convenient value, we now vary the toe and shoulder joints to the right and left. The effect of moving the toe is to raise and lower the lower spike of the zero discriminant along the incline of f, as shown in Figure D1(d), in Appendix D. As this spike passes through the diagonal, D, the two critical points annihilate. The periodic attractor, originally created from one of these by a Hopf bifurcation, eventually disappears (becomes nonattractive) as well, as shown in Fig. D1(e).

Similarly, moving the shoulder joint of e to the right lowers the upper spike along the incline parallel to f, as shown in Fig. D2(d). When this spike passes through the diagonal, D, another static annihilation catastrophe occurs. Taking these events together, we see that we have a static cusp catastrophe, with toe and shoulder joint hormonal concentrations as control parameters.

If the slope of f were above the Hopf bifurcation value (-8), this cusp catastrophe would involves two point attractors and a saddle point, the static cusp catastrophe. If the slope of f is below the Hopf bifurcation value but close to it (which it was not, in our simulations) then the two periodic attractors and the periodic saddle cycle would also be related in a cusp catastrophe, the periodic cusp catastrophe. Likewise, if the skirt of f were lifted as in Section 3 above, we conjecture that three chaotic limit sets (two attractors and a saddle) would be related in a chaotic cusp catastrophe. We have not verified this behavior with simulations, but the computer drawings of Appendix D are highly suggestive.

8. CONCLUSIONS

In the literature of complex dynamics (Abraham, 1982, 1983) it is proposed that serial networks of dynamical schemes provide a useful strategy for the architect of dynamical models and applications. Further, it is suggested that serial chains are important cases, and serial cycles are most important. The basic model of Smith (1981) was chosen as a test case for the theory. Here, we have put these proposals to a practical test. This results in a plausible modification to the basic model, a serial cycle with three dynamic nodes (Fig. 1), through the addition of one edge (Fig. 7). Simulations of the resulting complex dynamical scheme, exploring the effects of variations in its five parameters, reveal a rich bifurcation diagram. The qualitative interpretation of this diagram may enable better modeling and simulation of endocrine systems, and the discovery of new therapeutic strategies. Further, the application of this style of modeling to other kinds of complex systems may likewise create models for them, in which the basic phenomena of complex dynamics (chaos, intermittency, catastrophes, hysteresis, and so on) may be fitted by the model.

APPENDICES: COMPUTER DRAWN ORBITS

These are computer plots of two-dimensional projections of trajectories of the dynamical models into the (x,z) plane. They have been computed on a DEC VAX 11/780 with 2.5MB of main memory, and a floating point accelerator. The ORBIT program, written in C and run under UNIX V7/4.1BSD, uses a fourth-order Runge-Kutta algorithm with Richardson extrapolation. The output was viewed on a Ramtek 610 color graphics terminal (320×240 pixel resolution) and plotted on a Tektronix plotter.

A. BASIC MODEL, HOPF BIFURCATIONS.

Fig. A1. BASIC MODEL, STATIC DOMAIN.
The normal point attractor.
(a) Long feedback function.
(b) Short feedback function.
(c) Zero discriminant and diagonal.
(d) Detail of the intersection.
(e) Trajectories.

Fig. A2. BASIC MODEL, PERIODIC DOMAIN.
The normal periodic attractor.
(a) Long feedback function.
(b) Short feedback function.
(c) Zero discriminant and diagonal.
(d) Detail of the intersection.
(e) Trajectories.

B. RAISED SKIRT MODEL, ONSET OF CHAOS.

Fig. B1. RAISED SKIRT MODEL, PERIODIC DOMAIN.
The perturbed periodic attractor.
(a) Long feedback function.
(b) Short feedback function.
(c) Zero discriminant and diagonal.
(d) Detail of the intersection.
(e) Trajectories

Fig. B2. RAISED SKIRT MODEL, TRIPLE-PERIODIC DOMAIN.
Attractive cycle exhibiting triple the normal period.
(a) Long feedback function.
(b) Short feedback function.
(c) Zero discriminant and diagonal.
(d) Detail of the intersection.
(e) Trajectories.

Fig. B3. RAISED SKIRT MODEL, CHAOTIC DOMAIN.
The chaotic attractor of Rössler et al.
(a) Long Feedback function.
(b) Short feedback function.
(c) Zero discriminant and diagonal.
(d) Detail of the intersection.
(e) Trajectories.

C. SHORT FEEDBACK MODEL, BIRHYTHMICITY.

Fig. C1. SHORT FEEDBACK MODEL, BIMODAL DOMAIN.
The normal periodic attractor dominates, but a new point attractor has been born.
(a) Long feedback function.
(b) Short feedback function.
(c) Zero discriminant and diagonal.
(d) Detail of the intersection.
(e) Trajectories.

Fig. C2. SHORT FEEDBACK MODEL, BIRHYTHMIC DOMAIN
The new periodic attractor, inside the normal cycle, has appeared after a Hopf bifurcation of the new point attractor.
(a) Long feedback function.
(b) Short feedback function.
(c) Zero discriminant and diagonal.
(d) Detail of the intersection.
(e) Trajectories.

Fig. C3. SHORT FEEDBACK MODEL, ALTERNATE-PERIODIC DOMAIN.
The normal periodic attractor has destabilized, but the alternate periodic attractor remains.

(a) Long feedback function.
(b) Short feedback function.
(c) Zero discriminant and diagonal.
(d) Detail of the intersection.
(e) Trajectories.

Fig. C4. SHORT FEEDBACK MODEL, ALTERNATE-STATIC DOMAIN.
The alternate periodic attractor has become a point attractor, through an inverse Hopf bifucation.
(a) Long feedback function.
(b) Short feedback function.
(c) Zero discriminant and diagonal.
(d) Detail of the intersection.
(e) Trajectories.

D. SHORT FEEDBACK MODEL, CUSP CATASTROPHES.

Fig. D1. SHORT FEEDBACK MODEL, VARIATION OF THE TOE PARAMETER.
Compare with Fig. C2(e). Moving the toe to the left moves the lower spike upwards, along the incline of f, as shown in Fig. D1(d) here. In this case, the normal cycle has suffered a periodic annihilation catastrophe, involving a collision with its separator.
(a) Long feedback function.
(b) Short feedback function.
(c) Zero discriminant and diagonal.
(d) Detail of the intersection.
(e) Trajectories.

Fig. D2. SHORT FEEDBACK MODEL, VARIATION OF THE SHOULDER PARAMETER.
Compare with Fig. C2. Moving the shoulder to the right lowers the upper spike along the incline parallel to f, as shown in (d) here. In this case, the alternate limit cycle has become a perodic repellor.
(a) Long feedback function.
(b) Short feedback function.
(c) Zero discriminant and diagonal.
(d) Detail of the intersection.
(e) Trajectories.

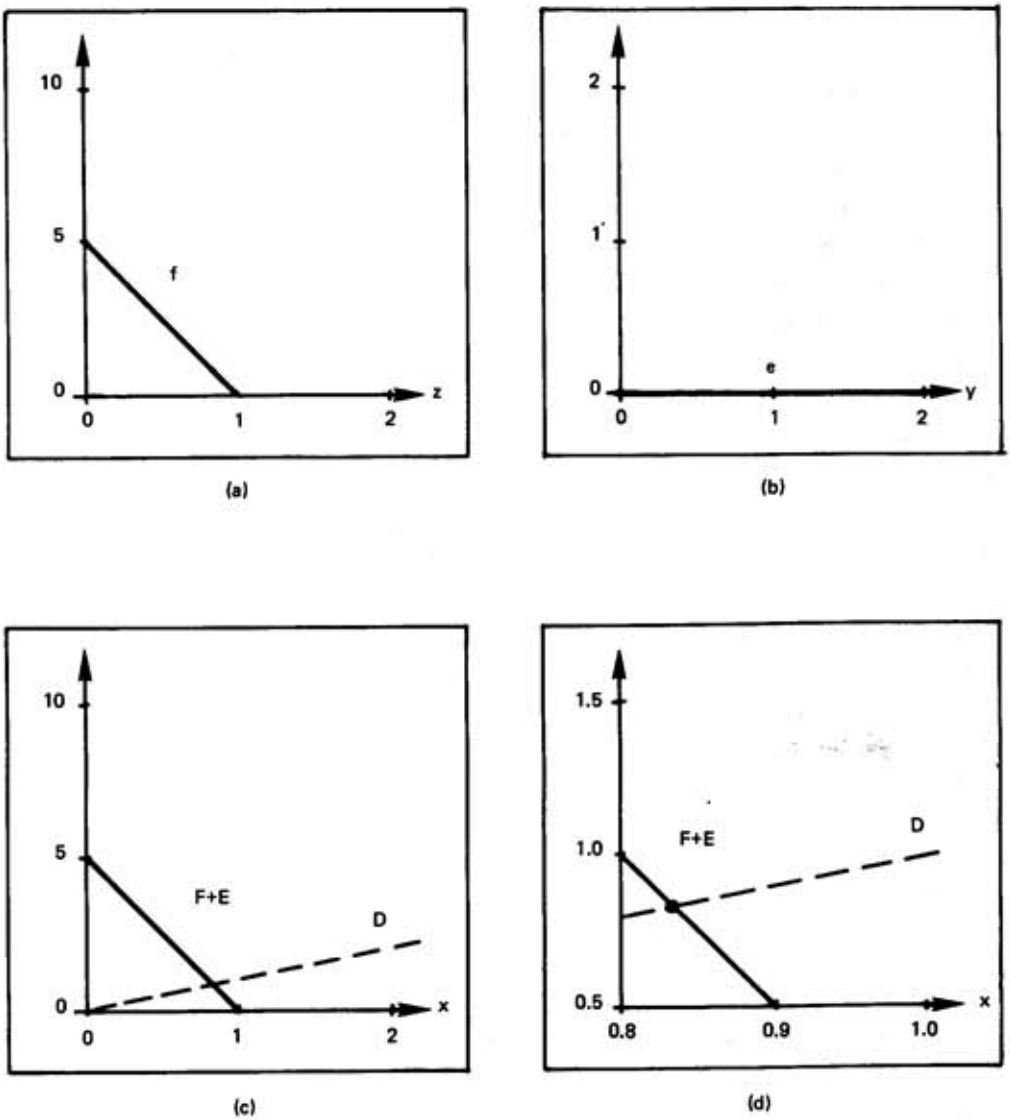

Fig. A1. BASIC MODEL, STATIC DOMAIN.

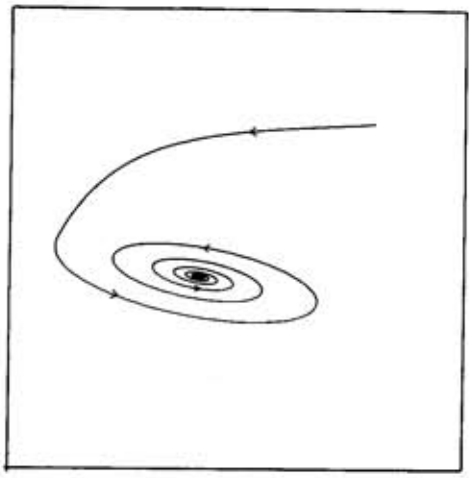

(e)

Fig. A1. BASIC MODEL, STATIC DOMAIN.
The normal point attractor.
(a) Long feedback function.
(b) Short feedback function.
(c) Zero discriminant and diagonal.
(d) Detail of the intersection.
(e) Trajectories.

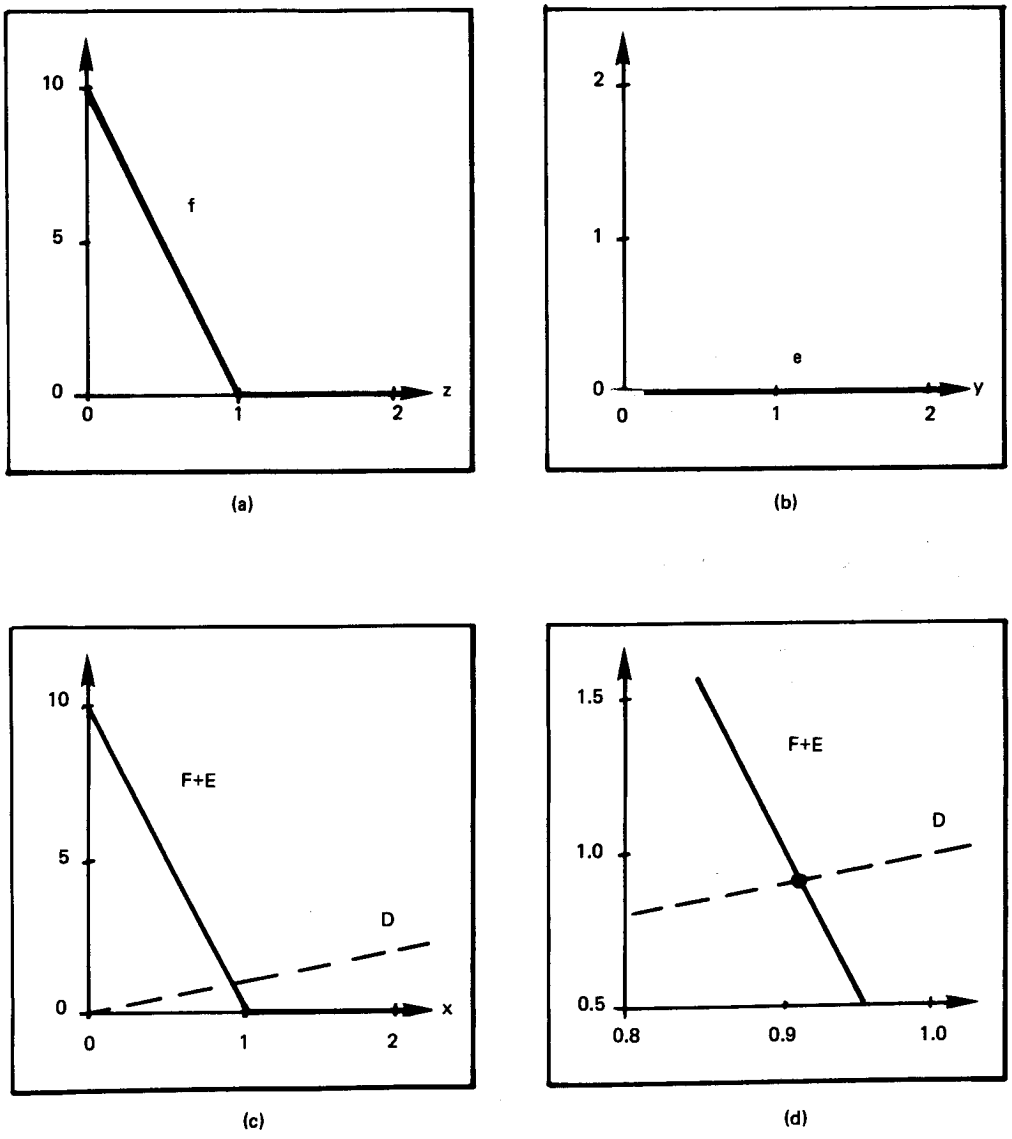

Fig. A2. BASIC MODEL, PERIODIC DOMAIN.

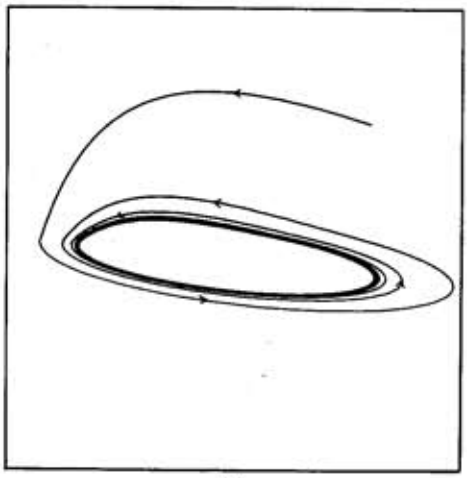

(e)

Fig. A2. BASIC MODEL, PERIODIC DOMAIN.
The normal periodic attractor.
(a) Long feedback function.
(b) Short feedback function.
(c) Zero discriminant and diagonal.
(d) Detail of the intersection.
(e) Trajectories.

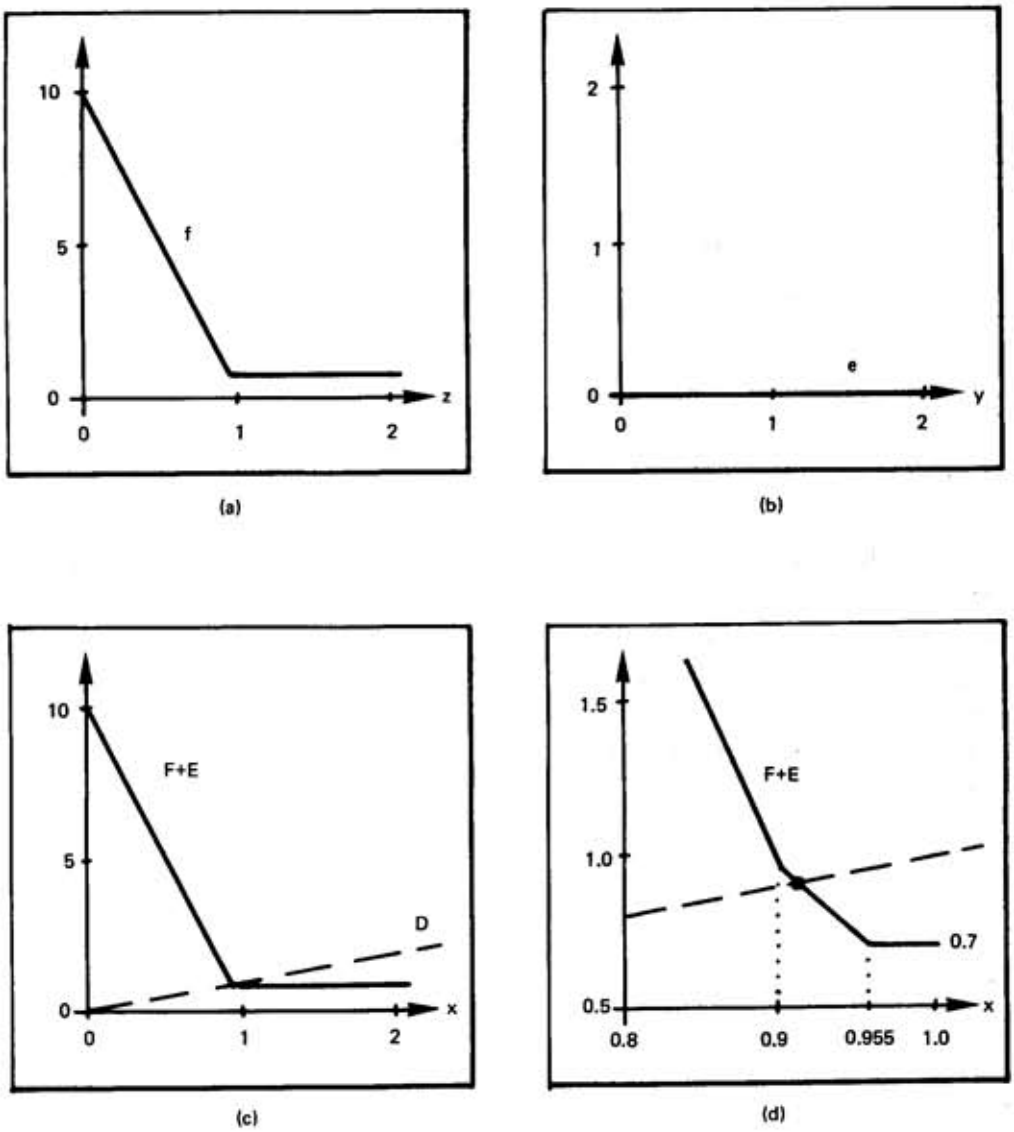

Fig. B1. RAISED SKIRT MODEL, PERIODIC DOMAIN.

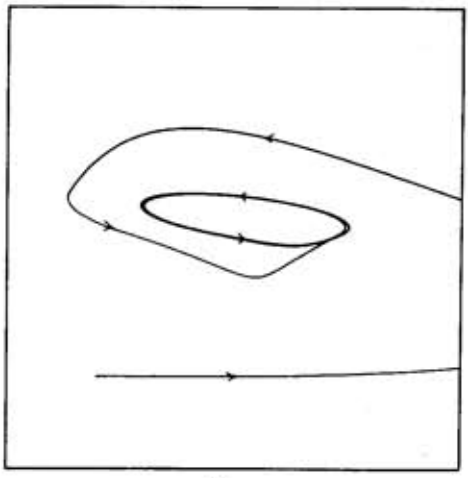

(e)

Fig. B1. RAISED SKIRT MODEL, PERIODIC DOMAIN.
The perturbed periodic attractor.
(a) Long feedback function.
(b) Short feedback function.
(c) Zero discriminant and diagonal.
(d) Detail of the intersection.
(e) Trajectories.

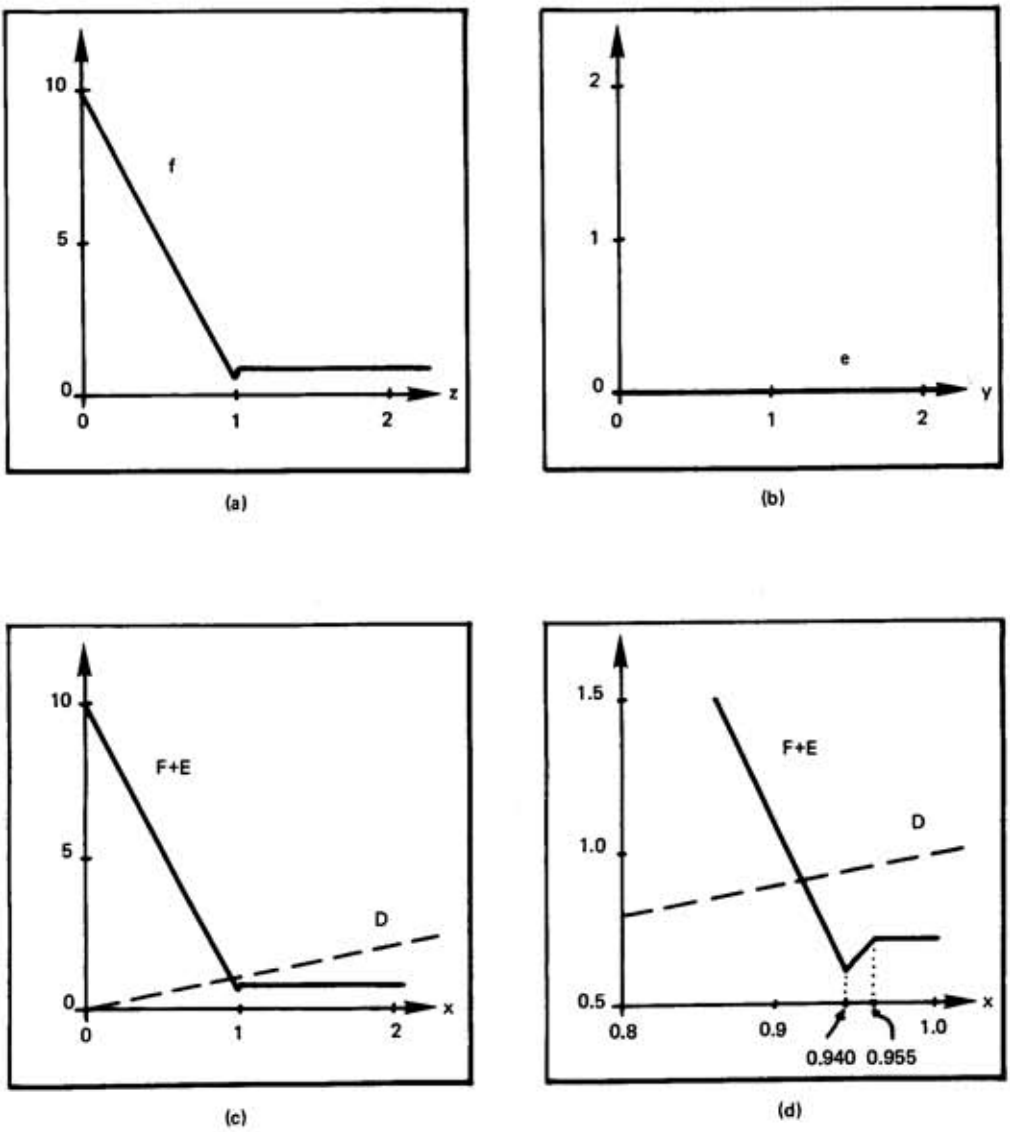

Fig. B2. RAISED SKIRT MODEL, TRIPLE-PERIODIC DOMAIN.

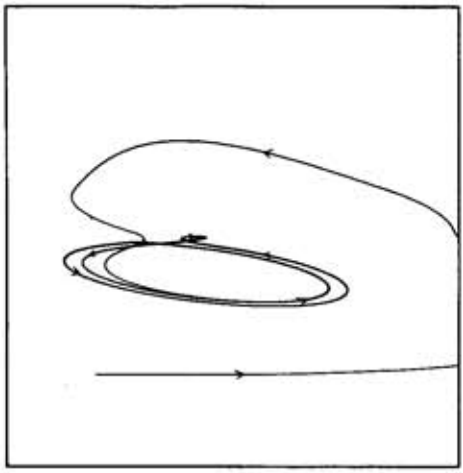

Fig. B2. RAISED SKIRT MODEL, TRIPLE-PERIODIC DOMAIN.
Attractive cycle exhibiting triple the normal period.
(a) Long feedback function.
(b) Short feedback function.
(c) Zero discriminant and diagonal.
(d) Detail of the intersection.
(e) Trajectories.

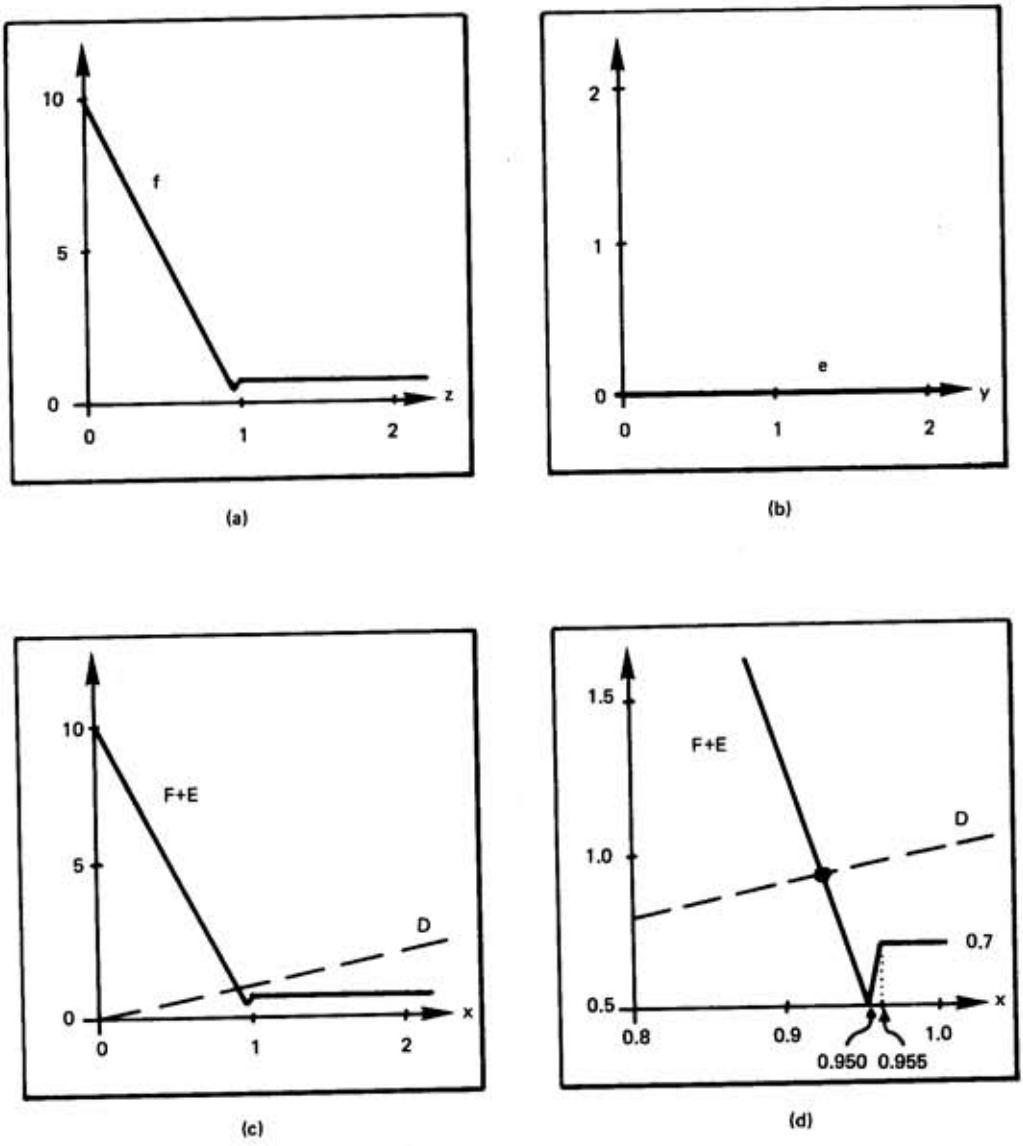

Fig. B3. RAISED SKIRT MODEL, CHAOTIC DOMAIN.

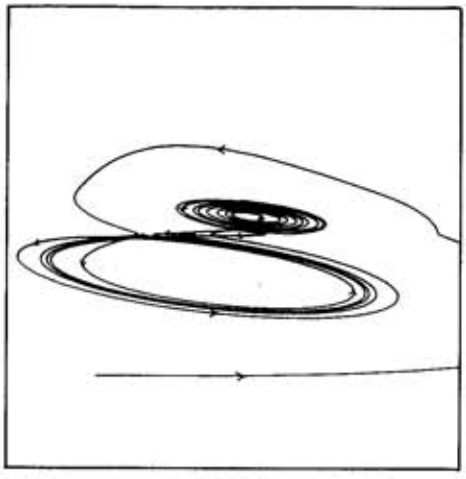

(e)

Fig. B3. RAISED SKIRT MODEL, CHAOTIC DOMAIN.
The chaotic attractor of Rössler et al.
(a) Long Feedback function.
(b) Short feedback function.
(c) Zero discriminant and diagonal.
(d) Detail of the intersection.
(e) Trajectories.

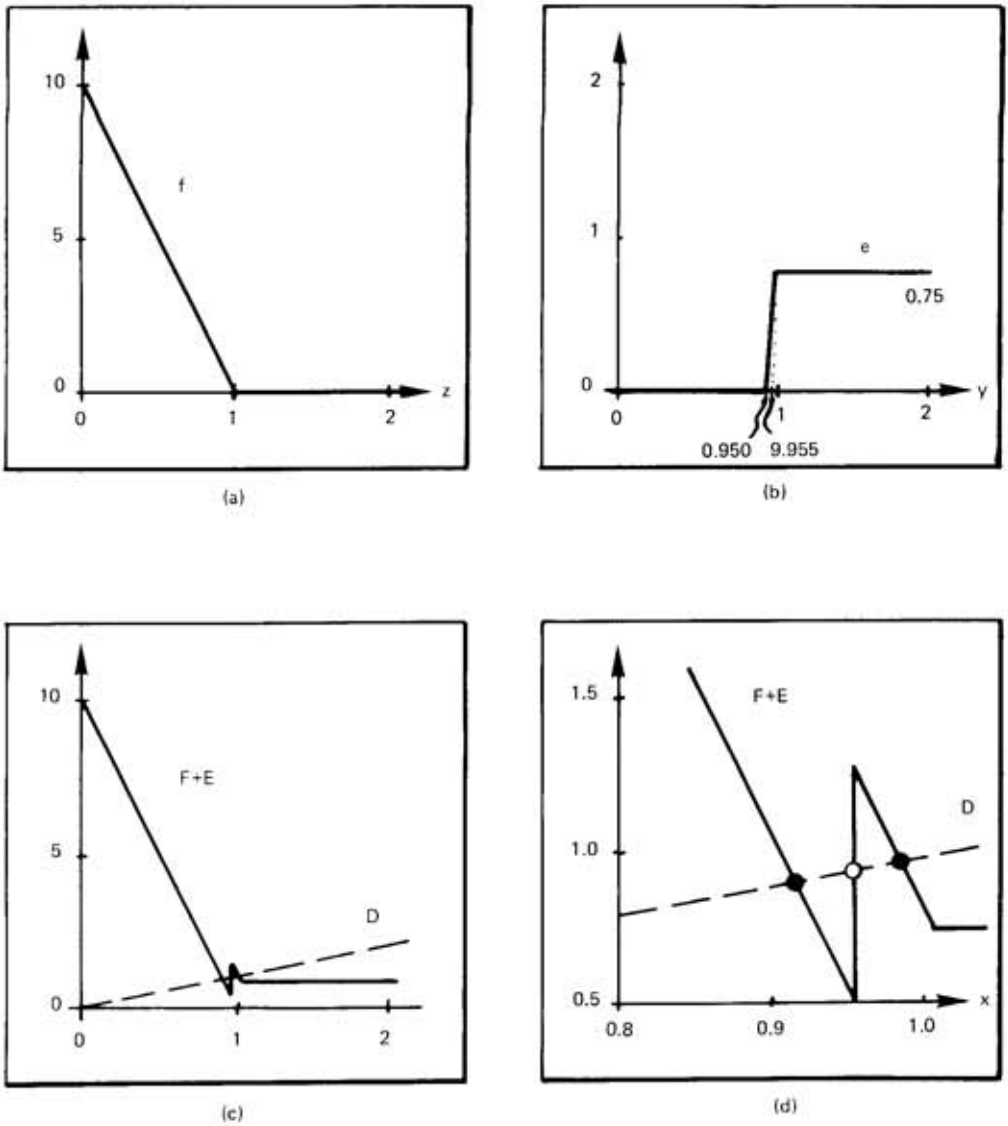

Fig. C1. SHORT FEEDBACK MODEL, BIMODAL DOMAIN.

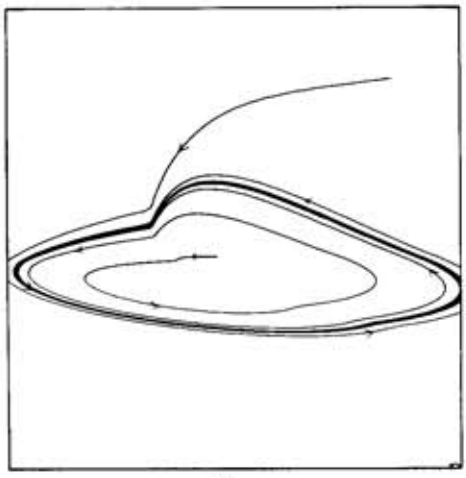

(e)

Fig. C1. SHORT FEEDBACK MODEL, BIMODAL DOMAIN.
The normal periodic attractor dominates, but a new point attractor has been born.

(a) Long feedback function.

(b) Short feedback function.

(c) Zero discriminant and diagonal.

(d) Detail of the intersection.

(e) Trajectories.

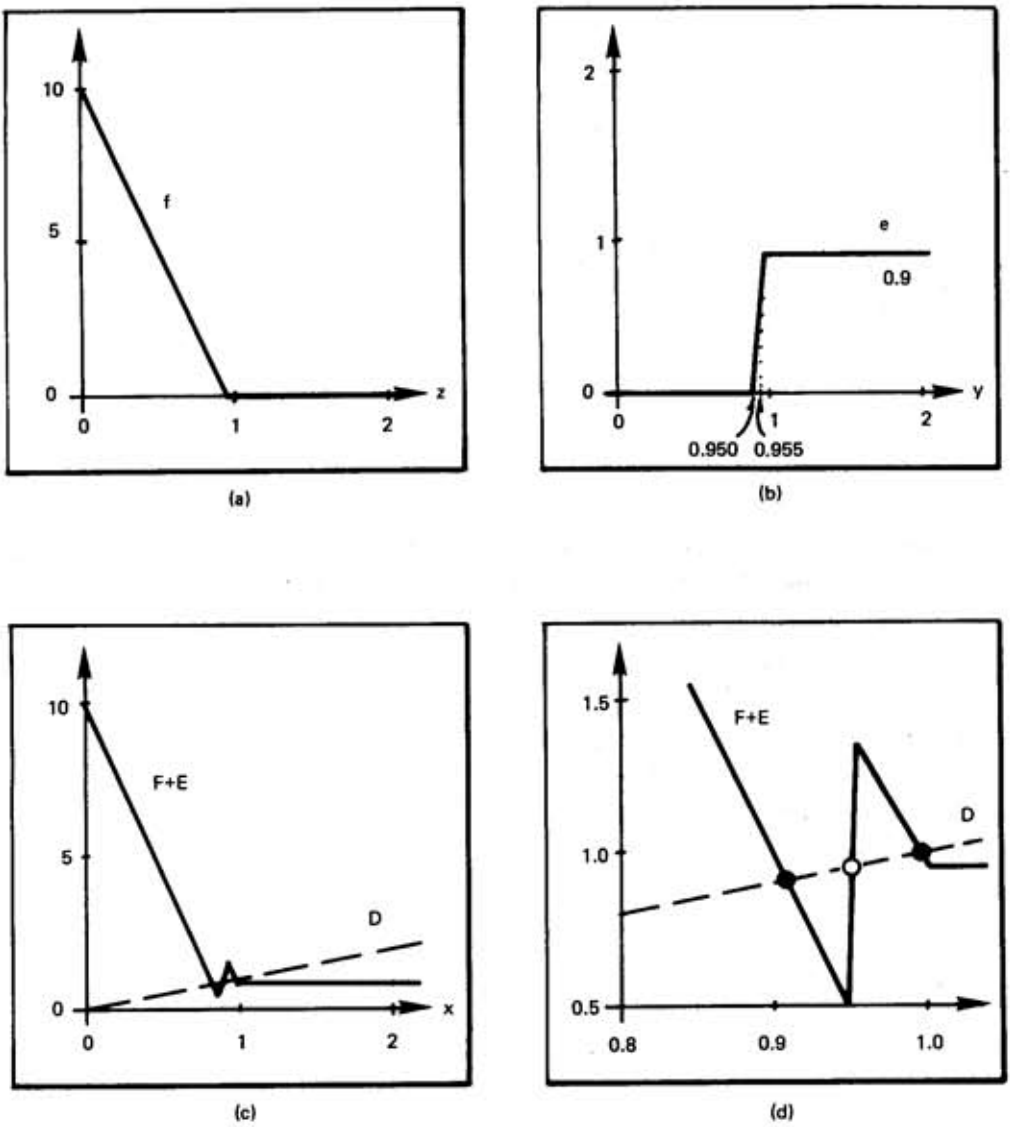

Fig. C2. SHORT FEEDBACK MODEL, BIRHYTHMIC DOMAIN

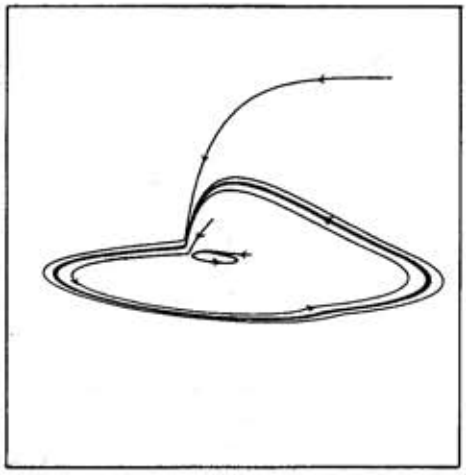

(e)

Fig. C2. SHORT FEEDBACK MODEL, BIRHYTHMIC DOMAIN

The new periodic attractor, inside the normal cycle, has appeared after a Hopf bifurcation of the new point attractor.

(a) Long feedback function.

(b) Short feedback function.

(c) Zero discriminant and diagonal.

(d) Detail of the intersection.

(e) Trajectories.

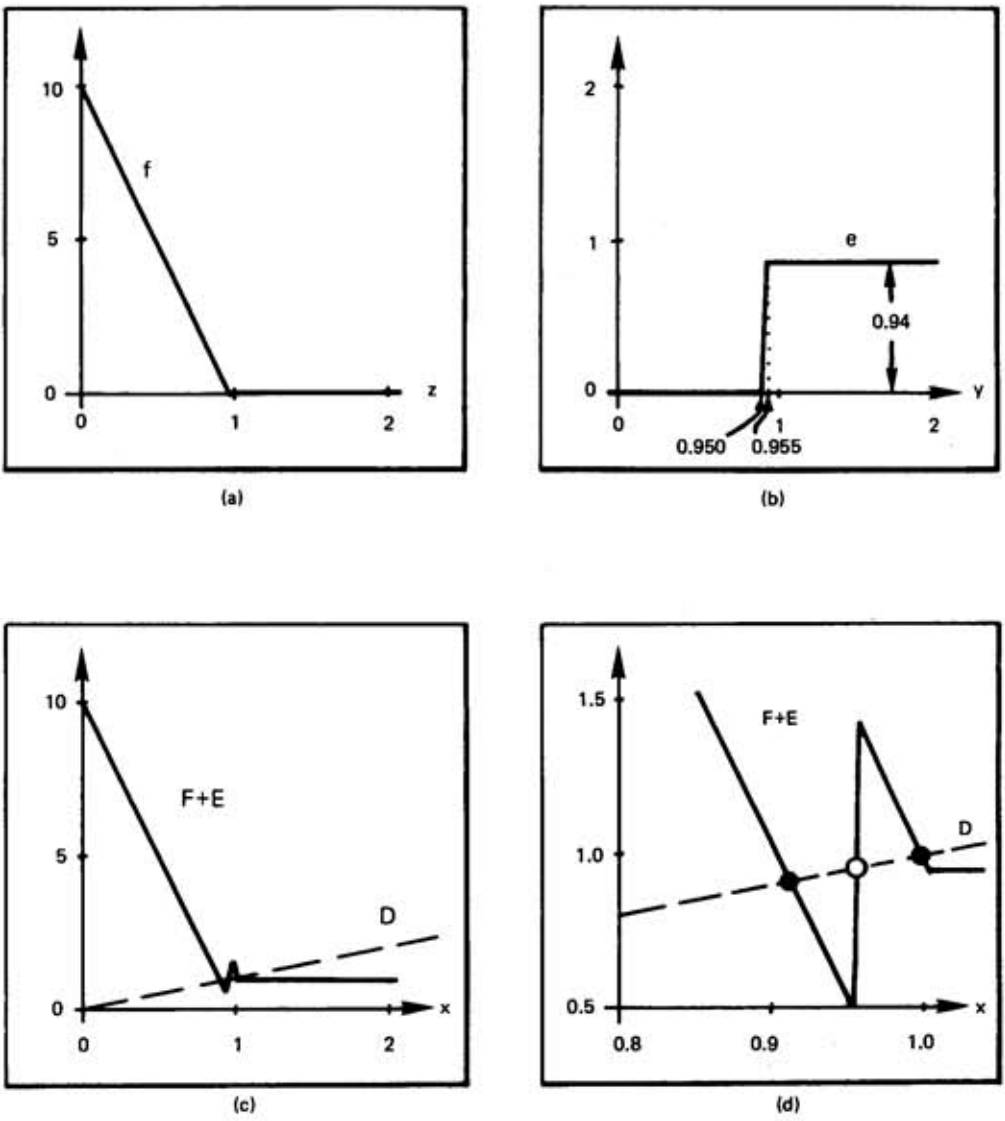

Fig. C3. SHORT FEEDBACK MODEL, ALTERNATE-PERIODIC DOMAIN.

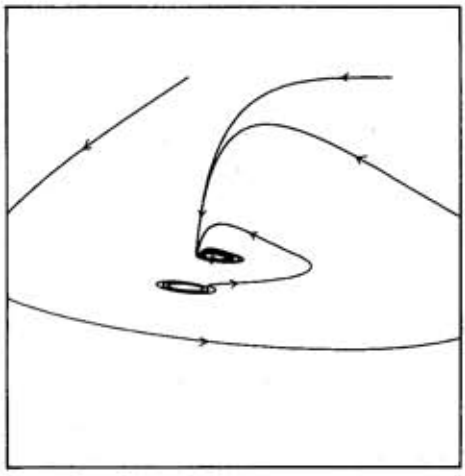

(e)

Fig. C3. SHORT FEEDBACK MODEL, ALTERNATE-PERIODIC DOMAIN.
The normal periodic attractor has destabilized, but the alternate periodic attractor remains.

(a) Long feedback function.

(b) Short feedback function.

(c) Zero discriminant and diagonal.

(d) Detail of the intersection.

(e) Trajectories.

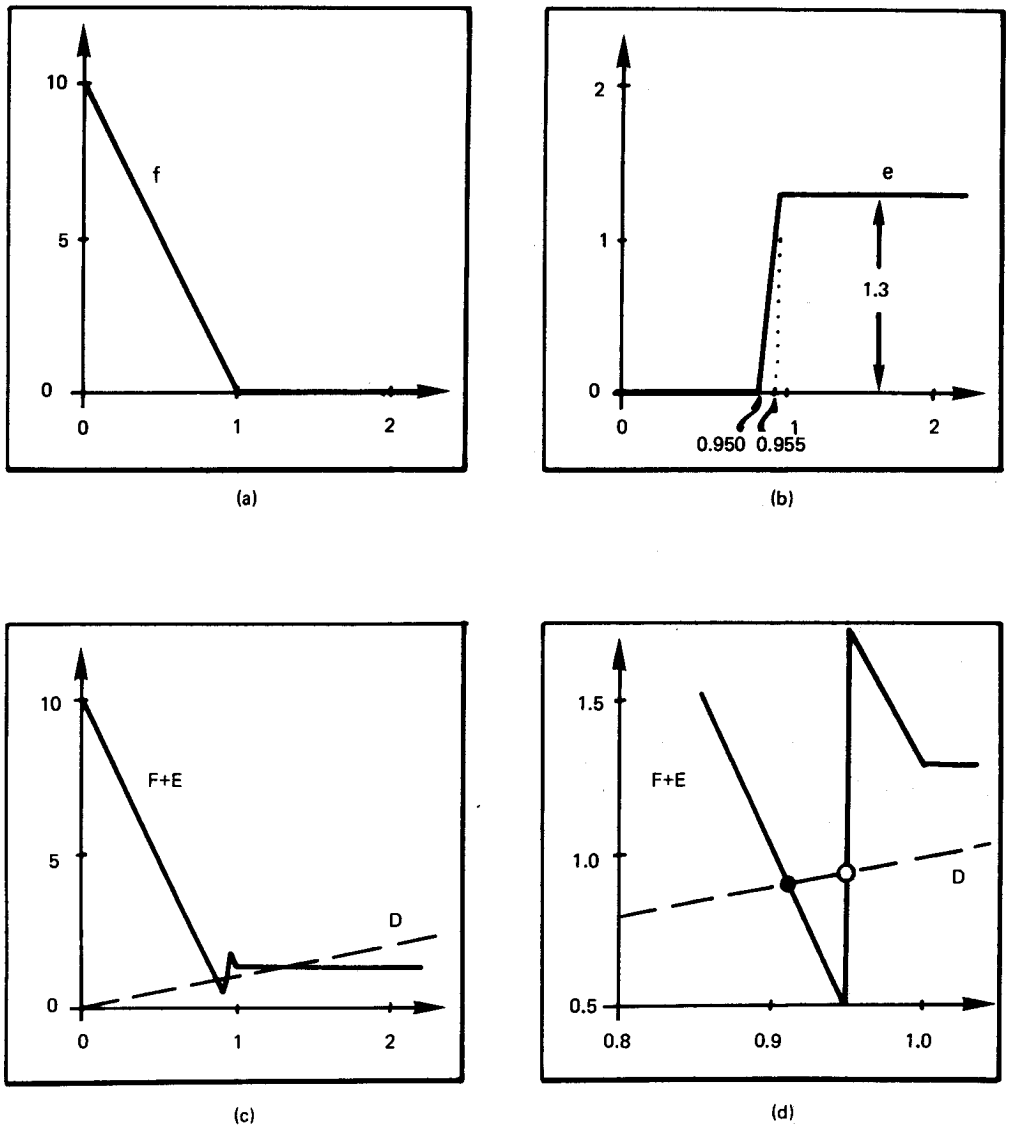

Fig. C4. SHORT FEEDBACK MODEL, ALTERNATE-STATIC DOMAIN.

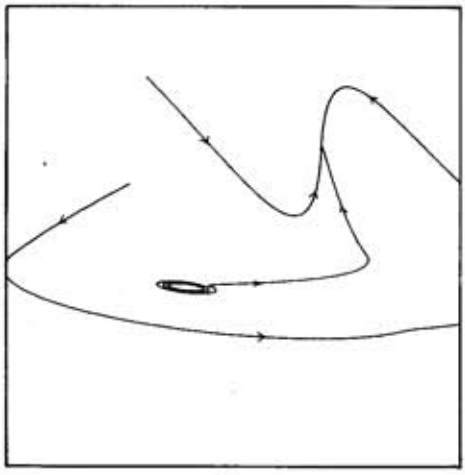

Fig. C4. SHORT FEEDBACK MODEL, ALTERNATE-STATIC DOMAIN.
The alternate periodic attractor has become a point attractor, through an inverse Hopf bifucation.
(a) Long feedback function.
(b) Short feedback function.
(c) Zero discriminant and diagonal.
(d) Detail of the intersection.
(e) Trajectories.

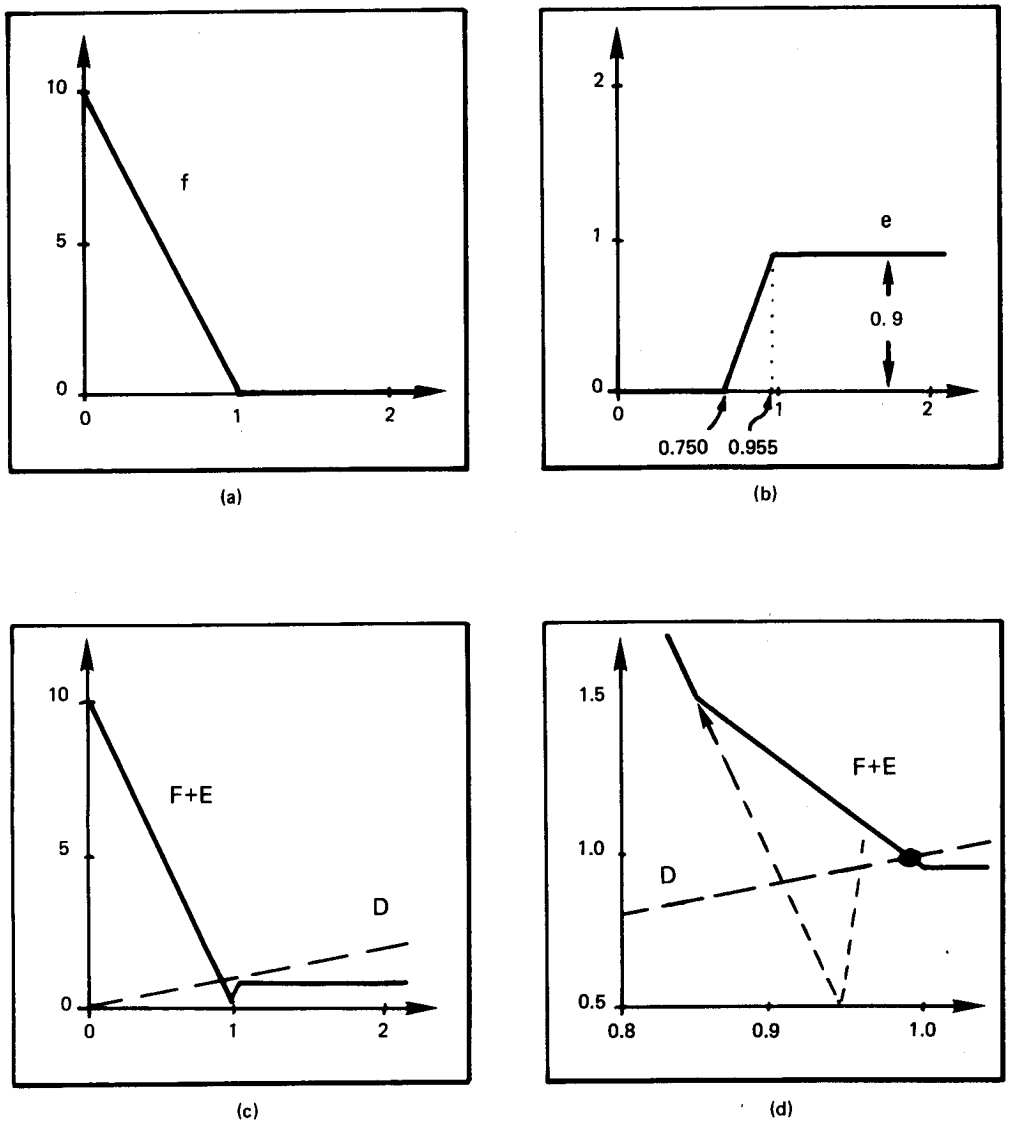

Fig. D1. SHORT FEEDBACK MODEL, VARIATION OF THE TOE PARAMETER.

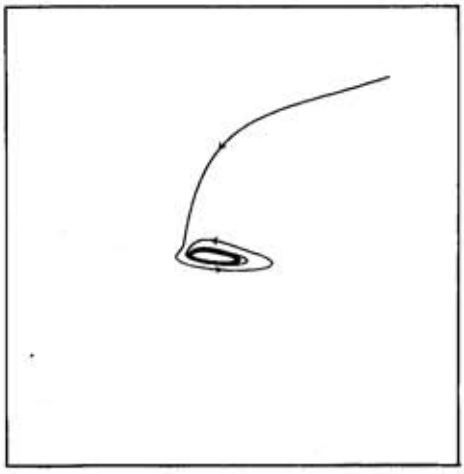

(e)

Fig. D1. SHORT FEEDBACK MODEL, VARIATION OF THE TOE PARAMETER. Compare with Fig. C2(e). Moving the toe to the left moves the lower spike upwards, along the incline of f, as shown in Fig. D1(d) here. In this case, the normal cycle has suffered a periodic annihilation catastrophe, involving a collision with its separator.

(a) Long feedback function.

(b) Short feedback function.

(c) Zero discriminant and diagonal.

(d) Detail of the intersection.

(e) Trajectories.

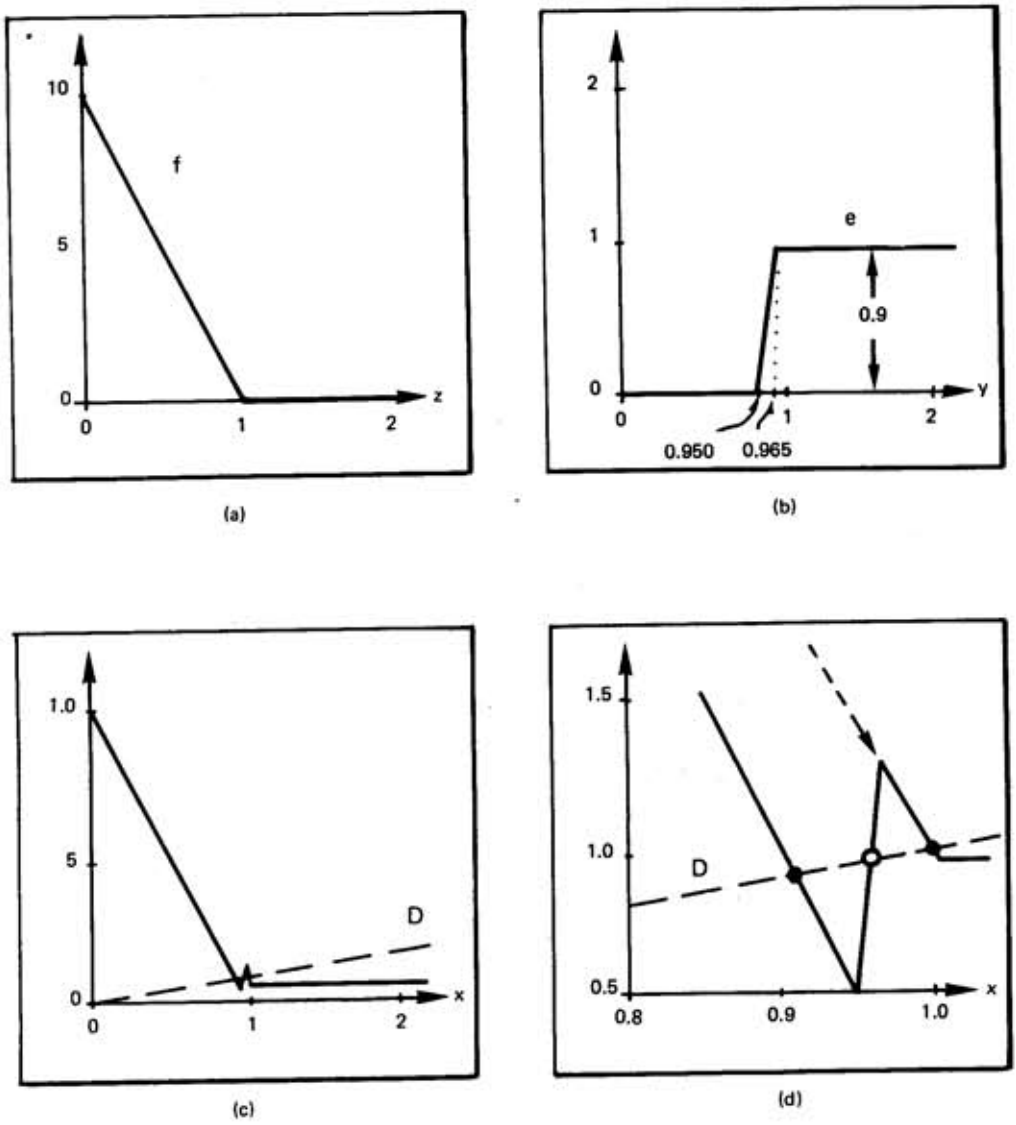

Fig. D2. SHORT FEEDBACK MODEL, VARIATION OF THE SHOULDER PARAMETER.

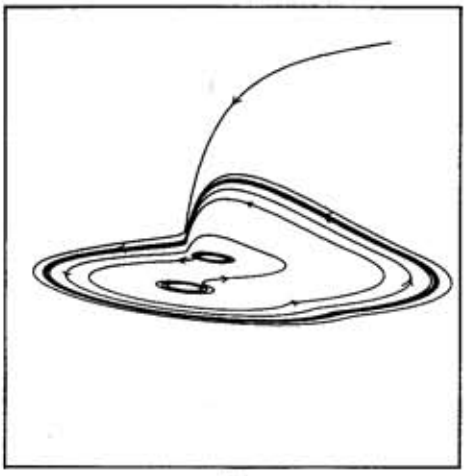

(e)

Fig. D2. SHORT FEEDBACK MODEL, VARIATION OF THE SHOULDER PARAMETER.

Compare with Fig. C2. Moving the shoulder to the right lowers the upper spike along the incline parallel to f, as shown in (d) here. In this case, the alternate limit cycle has become a perodic repellor.

(a) Long feedback function.

(b) Short feedback function.

(c) Zero discriminant and diagonal.

(d) Detail of the intersection.

(e) Trajectories.

ACKNOWLEDGEMENTS

This work was born in Guelph, and clearly owes much to Otto Rössler at the conference in March, 1981. The modified system resulted from further discussions in Guelph and Tübingen. The computer simulations were done in Santa Cruz, using the ORBIT software created by Ralph Abraham and Tod Blume, and adapted to this problem with the help of Bob Lansdon. We are grateful to Arthur Fischer, Otto Rössler and Alan Garfinkel for helpful conversations, and to the Universities of California, Guelph, and Tübingen for their support and hospitality during this project.

BIBLIOGRAPHY

Abraham, R. H., 1983a. Categories of dynamical models, in: T. M. Rassias (ed.), Global Analysis-Analysis on Manifolds, Teubner, Leibzig (in press).

Abraham, R. H., 1983b. Dynamical models for physiology, preprint.

Abraham, R. H., 1983c. Chaostrophes, Intermittency, and Noise, this volume.

Abraham, R. H. and C. D. Shaw, 1982. Dynamics, the Geometry of Behavior, Part 1: Periodic Behavior, Aerial Press, Box 1360, Santa Cruz, CA 95061.

Abraham, R. H. and C. D. Shaw, 1983. Dynamics, a visual introduction, in: F. E. Yates (ed.), Self-Organizing Systems, Plenum, (to appear).

Decroly, A. and A. Goldbeter, 1982. Birhythmicity, chaos, and other patterns of temporal self-organization in a multiply regulated biochemical system, Proc. Natl. Acad. Sci. USA 79: 6917-6921.

Jaffe, R. B., 1982. Pump that helps women ovulate, San Francisco Chronicle, p. 4, Sept. 10, 1982.

Rössler, R., R. G. Gotz, and O. E. Rössler, 1979. Chaos in endocrinology, Biophys. J. 25: 216(a).

Smith, W. R., 1981. Hypothalamic regulation of pituitary secretion of luteinizing hormone. II. Feedback control of gonadotropin secretion. Bull. Math. Biol. 42:57.

Sparrow, C. T., 1981. Chaos in a three-dimensional single loop feedback system with a piecewise linear feedback function, J. Math. Anal. Appl. 83: 275-291.